

Study of the $h_c(1^1P_1)$ meson via $\psi(2S) \rightarrow \pi^0 h_c$ decays at BESIII

M. Ablikim¹, M. N. Achasov^{10,b}, P. Adlarson⁶⁸, S. Ahmed¹⁴, M. Albrecht⁴, R. Aliberti²⁸, A. Amoroso^{67A,67C}, M. R. An³², Q. An^{64,50}, X. H. Bai⁵⁸, Y. Bai⁴⁹, O. Bakina²⁹, R. Baldini Ferroli^{23A}, I. Balossino^{24A}, Y. Ban^{39,h}, V. Batozskaya^{1,37}, D. Becker²⁸, K. Begzsuren²⁶, N. Berger²⁸, M. Bertani^{23A}, D. Bettoni^{24A}, F. Bianchi^{67A,67C}, J. Bloms⁶¹, A. Bortone^{67A,67C}, I. Boyko²⁹, R. A. Briere⁵, A. Brueggemann⁶¹, H. Cai⁶⁹, X. Cai^{1,50}, A. Calcaterra^{23A}, G. F. Cao^{1,55}, N. Cao^{1,55}, S. A. Cetin^{54A}, J. F. Chang^{1,50}, W. L. Chang^{1,55}, G. Chelkov^{29,a}, C. Chen³⁶, G. Chen¹, H. S. Chen^{1,55}, M. L. Chen^{1,50}, S. J. Chen³⁵, T. Chen¹, X. R. Chen²⁵, X. T. Chen¹, Y. B. Chen^{1,50}, Z. J. Chen^{20,i}, W. S. Cheng^{67C}, G. Cibinetto^{24A}, F. Cossio^{67C}, J. J. Cui⁴², H. L. Dai^{1,50}, J. P. Dai⁷¹, A. Dbeyssi¹⁴, R. E. de Boer⁴, D. Dedovich²⁹, Z. Y. Deng¹, A. Denig²⁸, I. Denysenko²⁹, M. Destefanis^{67A,67C}, F. De Mori^{67A,67C}, Y. Ding³³, J. Dong^{1,50}, L. Y. Dong^{1,55}, M. Y. Dong^{1,50,55}, X. Dong⁶⁹, S. X. Du⁷³, P. Egorov^{29,a}, Y. L. Fan⁶⁹, J. Fang^{1,50}, S. S. Fang^{1,55}, Y. Fang¹, R. Farinelli^{24A}, L. Fava^{67B,67C}, F. Feldbauer⁴, G. Felici^{23A}, C. Q. Feng^{64,50}, J. H. Feng⁵¹, K. Fischer⁶², M. Fritsch⁴, C. D. Fu¹, Y. N. Gao^{39,h}, Yang Gao^{64,50}, I. Garzia^{24A,24B}, P. T. Ge⁶⁹, C. Geng⁵¹, E. M. Gersabeck⁵⁹, A. Gilman⁶², K. Goetzen¹¹, L. Gong³³, W. X. Gong^{1,50}, W. Gradl²⁸, M. Greco^{67A,67C}, M. H. Gu^{1,50}, C. Y. Guan^{1,55}, A. Q. Guo²⁵, A. Q. Guo²², L. B. Guo³⁴, R. P. Guo⁴¹, Y. P. Guo^{9,g}, A. Guskov^{29,a}, T. T. Han⁴², W. Y. Han³², X. Q. Hao¹⁵, F. A. Harris⁵⁷, K. K. He⁴⁷, K. L. He^{1,55}, F. H. Heinsius⁴, C. H. Heinz²⁸, Y. K. Heng^{1,50,55}, C. Herold⁵², M. Himmelreich^{11,e}, T. Holtmann⁴, G. Y. Hou^{1,55}, Y. R. Hou⁵⁵, Z. L. Hou¹, H. M. Hu^{1,55}, J. F. Hu^{48,j}, T. Hu^{1,50,55}, Y. Hu¹, G. S. Huang^{64,50}, K. X. Huang⁵¹, L. Q. Huang⁶⁵, X. T. Huang⁴², Y. P. Huang¹, Z. Huang^{39,h}, T. Hussain⁶⁶, N. Hüsken^{22,28}, W. Imoehl²², M. Irshad^{64,50}, S. Jaeger⁴, S. Janchiv²⁶, Q. Ji¹, Q. P. Ji¹⁵, X. B. Ji^{1,55}, X. L. Ji^{1,50}, Y. Y. Ji⁴², H. B. Jiang⁴², S. S. Jiang³², X. S. Jiang^{1,50,55}, J. B. Jiao⁴², Z. Jiao¹⁸, S. Jin³⁵, Y. Jin⁵⁸, M. Q. Jing^{1,55}, T. Johansson⁶⁸, N. Kalantar-Nayestanaki⁵⁶, X. S. Kang³³, R. Kappert⁵⁶, M. Kavatsyuk⁵⁶, B. C. Ke⁷³, I. K. Keshk⁴, A. Khoukaz⁶¹, P. Kiese²⁸, R. Kiuchi¹, R. Klemt¹¹, L. Koch³⁰, O. B. Kolcu^{54A}, B. Kopf⁴, M. Kuemmel⁴, M. Kuessner⁴, A. Kupsc^{37,68}, W. Kühn³⁰, J. J. Lane⁵⁹, J. S. Lange³⁰, P. Larin¹⁴, A. Lavania²¹, L. Lavezzi^{67A,67C}, Z. H. Lei^{64,50}, H. Leithoff²⁸, M. Lellmann²⁸, T. Lenz²⁸, C. Li⁴⁰, C. Li³⁶, C. H. Li³², Cheng Li^{64,50}, D. M. Li⁷³, F. Li^{1,50}, G. Li¹, H. Li^{64,50}, H. Li⁴⁴, H. B. Li^{1,55}, H. J. Li¹⁵, H. N. Li^{48,j}, J. L. Li⁴², J. Q. Li⁴, J. S. Li⁵¹, Ke Li¹, L. J. Li¹, L. K. Li¹, Lei Li³, M. H. Li³⁶, P. R. Li^{31,k,l}, S. X. Li⁹, S. Y. Li⁵³, T. Li⁴², W. D. Li^{1,55}, W. G. Li¹, X. H. Li^{64,50}, X. L. Li⁴², Xiaoyu Li^{1,55}, Z. Y. Li⁵¹, H. Liang²⁷, H. Liang^{64,50}, H. Liang^{1,55}, Y. F. Liang⁴⁶, Y. T. Liang²⁵, G. R. Liao¹², J. Libby²¹, A. Limphirat⁵², C. X. Lin⁵¹, D. X. Lin²⁵, T. Lin¹, B. J. Liu¹, C. X. Liu¹, D. Liu^{14,64}, F. H. Liu⁴⁵, Fang Liu¹, Feng Liu⁶, G. M. Liu^{48,j}, H. M. Liu^{1,55}, Huanhuan Liu¹, Huihui Liu¹⁶, J. B. Liu^{64,50}, J. L. Liu⁶⁵, J. Y. Liu^{1,55}, K. Liu¹, K. Y. Liu³³, Ke Liu¹⁷, L. Liu^{64,50}, M. H. Liu^{9,g}, P. L. Liu¹, Q. Liu⁵⁵, S. B. Liu^{64,50}, T. Liu^{9,g}, W. M. Liu^{64,50}, X. Liu^{31,k,l}, Y. Liu^{31,k,l}, Y. B. Liu³⁶, Z. A. Liu^{1,50,55}, Z. Q. Liu⁴², X. C. Lou^{1,50,55}, F. X. Lu⁵¹, H. J. Lu¹⁸, J. G. Lu^{1,50}, X. L. Lu¹, Y. Lu¹, Y. P. Lu^{1,50}, Z. H. Lu¹, C. L. Luo³⁴, M. X. Luo⁷², T. Luo^{9,g}, X. L. Luo^{1,50}, X. R. Lyu⁵⁵, Y. F. Lyu³⁶, F. C. Ma³³, H. L. Ma¹, L. L. Ma⁴², M. M. Ma^{1,55}, Q. M. Ma¹, R. Q. Ma^{1,55}, R. T. Ma⁵⁵, X. Y. Ma^{1,50}, Y. Ma^{39,h}, F. E. Maas¹⁴, M. Maggiora^{67A,67C}, S. Maldaner⁴, S. Malde⁶², Q. A. Malik⁶⁶, A. Mangoni^{23B}, Y. J. Mao^{39,h}, Z. P. Mao¹, S. Marcello^{67A,67C}, Z. X. Meng⁵⁸, J. G. Messchendorp^{56,d}, G. Mezzadri^{24A}, H. Miao¹, T. J. Min³⁵, R. E. Mitchell²², X. H. Mo^{1,50,55}, N. Yu. Muchnoi^{10,b}, H. Muramatsu⁶⁰, S. Nakhoul^{11,e}, Y. Nefedov²⁹, F. Nerling^{11,e}, I. B. Nikolaev^{10,b}, Z. Ning^{1,50}, S. Nisar^{8,m}, S. L. Olsen⁵⁵, Q. Ouyang^{1,50,55}, S. Pacetti^{23B,23C}, X. Pan^{9,g}, Y. Pan⁵⁹, A. Pathak¹, A. Pathak²⁷, M. Pelizaeus⁴, H. P. Peng^{64,50}, K. Peters^{11,e}, J. Pettersson⁶⁸, J. L. Ping³⁴, R. G. Ping^{1,55}, S. Plura²⁸, S. Pogodin²⁹, R. Poling⁶⁰, V. Prasad^{64,50}, H. Qi^{64,50}, H. R. Qi⁵³, M. Qi³⁵, T. Y. Qi^{9,g}, S. Qian^{1,50}, W. B. Qian⁵⁵, Z. Qian⁵¹, C. F. Qiao⁵⁵, J. J. Qin⁶⁵, L. Q. Qin¹², X. P. Qin^{9,g}, X. S. Qin⁴², Z. H. Qin^{1,50}, J. F. Qiu¹, S. Q. Qu⁵³, S. Q. Qu³⁶, K. H. Rashid⁶⁶, K. Ravindran²¹, C. F. Redmer²⁸, K. J. Ren³², A. Rivetti^{67C}, V. Rodin⁵⁶, M. Rolo^{67C}, G. Rong^{1,55}, Ch. Rosner¹⁴, M. Rump⁶¹, H. S. Sang⁶⁴, A. Sarantsev^{29,c}, Y. Schelhaas²⁸, C. Schnier⁴, K. Schoenning⁶⁸, M. Scodreggio^{24A,24B}, K. Y. Shan^{9,g}, W. Shan¹⁹, X. Y. Shan^{64,50}, J. F. Shanguan⁴⁷, L. G. Shao^{1,55}, M. Shao^{64,50}, C. P. Shen^{9,g}, H. F. Shen^{1,55}, X. Y. Shen^{1,55}, B.-A. Shi⁵⁵, H. C. Shi^{64,50}, R. S. Shi^{1,55}, X. Shi^{1,50}, X. D. Shi^{64,50}, J. J. Song¹⁵, W. M. Song^{27,1}, Y. X. Song^{39,h}, S. Sosio^{67A,67C}, S. Spataro^{67A,67C}, F. Stieler²⁸, K. X. Su⁶⁹, P. P. Su⁴⁷, Y.-J. Su⁵⁵, G. X. Sun¹, H. K. Sun¹, J. F. Sun¹⁵, L. Sun⁶⁹, S. S. Sun^{1,55}, T. Sun^{1,55}, W. Y. Sun²⁷, X. Sun^{20,i}, Y. J. Sun^{64,50}, Y. Z. Sun¹, Z. T. Sun⁴², Y. H. Tan⁶⁹, Y. X. Tan^{64,50}, C. J. Tang⁴⁶, G. Y. Tang¹, J. Tang⁵¹, L. Y. Tao⁶⁵, Q. T. Tao^{20,i}, J. X. Teng^{64,50}, V. Thoren⁶⁸, W. H. Tian⁴⁴, Y. T. Tian²⁵, I. Uman^{54B}, B. Wang¹, D. Y. Wang^{39,h}, F. Wang⁶⁵, H. J. Wang^{31,k,l}, H. P. Wang^{1,55}, K. Wang^{1,50}, L. L. Wang¹, M. Wang⁴², M. Z. Wang^{39,h}, Meng Wang^{1,55}, S. Wang^{9,g}, T. J. Wang³⁶, W. Wang⁵¹, W. H. Wang⁶⁹, W. P. Wang^{64,50}, X. Wang^{39,h}, X. F. Wang^{31,k,l}, X. L. Wang^{9,g}, Y. D. Wang³⁸, Y. F. Wang^{1,50,55}, Y. Q. Wang¹, Y. Y. Wang^{31,k,l}, Ying Wang⁵¹, Z. Wang^{1,50}, Z. Y. Wang¹, Ziyi Wang⁵⁵, D. H. Wei¹², F. Weidner⁶¹, S. P. Wen¹, D. J. White⁵⁹, U. Wiedner⁴, G. Wilkinson⁶², M. Wolke⁶⁸, L. Wollenberg⁴, J. F. Wu^{1,55}, L. H. Wu¹, L. J. Wu^{1,55}, X. Wu^{9,g}, X. H. Wu²⁷, Y. Wu⁶⁴, Z. Wu^{1,50}, L. Xia^{64,50}, T. Xiang^{39,h}, H. Xiao^{9,g}, S. Y. Xiao¹, Y. L. Xiao^{9,g}, Z. J. Xiao³⁴, X. H. Xie^{39,h}, Y. G. Xie^{1,50}, Y. H. Xie⁶, Z. P. Xie^{64,50}, T. Y. Xing^{1,55}, C. F. Xu¹, C. J. Xu⁵¹, G. F. Xu¹, Q. J. Xu¹³, S. Y. Xu⁶³, X. P. Xu⁴⁷, Y. C. Xu⁵⁵, F. Yan^{9,g}, L. Yan^{9,g}, W. B. Yan^{64,50}, W. C. Yan⁷³, H. J. Yang^{43,f}, H. X. Yang¹, L. Yang⁴⁴, S. L. Yang⁵⁵, Y. X. Yang^{1,55}, Yifan Yang^{1,55}, Zhi Yang²⁵, M. Ye^{1,50}, M. H. Ye⁷, J. H. Yin¹, Z. Y. You⁵¹, B. X. Yu^{1,50,55}, C. X. Yu³⁶, G. Yu^{1,55}, J. S. Yu^{20,i}, T. Yu⁶⁵, C. Z. Yuan^{1,55}, L. Yuan², S. C. Yuan¹, X. Q. Yuan¹, Y. Yuan¹, Z. Y. Yuan⁵¹, C. X. Yue³², A. A. Zafar⁶⁶, X. Zeng Zeng⁶, Y. Zeng^{20,i}, Y. H. Zhan⁵¹,

A. Q. Zhang¹, B. L. Zhang¹, B. X. Zhang¹, G. Y. Zhang¹⁵, H. Zhang⁶⁴, H. H. Zhang²⁷, H. H. Zhang⁵¹, H. Y. Zhang^{1,50},
 J. L. Zhang⁷⁰, J. Q. Zhang³⁴, J. W. Zhang^{1,50,55}, J. Y. Zhang¹, J. Z. Zhang^{1,55}, Jianyu Zhang^{1,55}, Jiawei Zhang^{1,55},
 L. M. Zhang⁵³, L. Q. Zhang⁵¹, Lei Zhang³⁵, P. Zhang¹, Shulei Zhang^{20,i}, X. D. Zhang³⁸, X. M. Zhang¹, X. Y. Zhang⁴⁷,
 X. Y. Zhang⁴², Y. Zhang⁶², Y. T. Zhang⁷³, Y. H. Zhang^{1,50}, Yan Zhang^{64,50}, Yao Zhang¹, Z. H. Zhang¹, Z. Y. Zhang⁶⁹,
 Z. Y. Zhang³⁶, G. Zhao¹, J. Zhao³², J. Y. Zhao^{1,55}, J. Z. Zhao^{1,50}, Lei Zhao^{64,50}, Ling Zhao¹, M. G. Zhao³⁶, Q. Zhao¹,
 S. J. Zhao⁷³, Y. B. Zhao^{1,50}, Y. X. Zhao²⁵, Z. G. Zhao^{64,50}, A. Zhemchugov^{29,a}, B. Zheng⁶⁵, J. P. Zheng^{1,50}, Y. H. Zheng⁵⁵,
 B. Zhong³⁴, C. Zhong⁶⁵, X. Zhong⁵¹, L. P. Zhou^{1,55}, X. Zhou⁶⁹, X. K. Zhou⁵⁵, X. R. Zhou^{64,50}, X. Y. Zhou³², Y. Z. Zhou^{9,g},
 J. Zhu³⁶, K. Zhu¹, K. J. Zhu^{1,50,55}, S. H. Zhu⁶³, T. J. Zhu⁷⁰, W. J. Zhu³⁶, W. J. Zhu^{9,g}, Y. C. Zhu^{64,50}, Z. A. Zhu^{1,55},
 B. S. Zou¹, J. H. Zou¹

(BESIII Collaboration)

¹ *Institute of High Energy Physics, Beijing 100049, People's Republic of China*

² *Beihang University, Beijing 100191, People's Republic of China*

³ *Beijing Institute of Petrochemical Technology, Beijing 102617, People's Republic of China*

⁴ *Bochum Ruhr-University, D-44780 Bochum, Germany*

⁵ *Carnegie Mellon University, Pittsburgh, Pennsylvania 15213, USA*

⁶ *Central China Normal University, Wuhan 430079, People's Republic of China*

⁷ *China Center of Advanced Science and Technology, Beijing 100190, People's Republic of China*

⁸ *COMSATS University Islamabad, Lahore Campus, Defence Road, Off Raiwind Road, 54000 Lahore, Pakistan*

⁹ *Fudan University, Shanghai 200433, People's Republic of China*

¹⁰ *G.I. Budker Institute of Nuclear Physics SB RAS (BINP), Novosibirsk 630090, Russia*

¹¹ *GSI Helmholtzcentre for Heavy Ion Research GmbH, D-64291 Darmstadt, Germany*

¹² *Guangxi Normal University, Guilin 541004, People's Republic of China*

¹³ *Hangzhou Normal University, Hangzhou 310036, People's Republic of China*

¹⁴ *Helmholtz Institute Mainz, Staudinger Weg 18, D-55099 Mainz, Germany*

¹⁵ *Henan Normal University, Xinxiang 453007, People's Republic of China*

¹⁶ *Henan University of Science and Technology, Luoyang 471003, People's Republic of China*

¹⁷ *Henan University of Technology, Zhengzhou 450001, People's Republic of China*

¹⁸ *Huangshan College, Huangshan 245000, People's Republic of China*

¹⁹ *Hunan Normal University, Changsha 410081, People's Republic of China*

²⁰ *Hunan University, Changsha 410082, People's Republic of China*

²¹ *Indian Institute of Technology Madras, Chennai 600036, India*

²² *Indiana University, Bloomington, Indiana 47405, USA*

²³ *INFN Laboratori Nazionali di Frascati, (A)INFN Laboratori Nazionali di Frascati, I-00044, Frascati, Italy; (B)INFN Sezione di Perugia, I-06100, Perugia, Italy; (C)University of Perugia, I-06100, Perugia, Italy*

²⁴ *INFN Sezione di Ferrara, (A)INFN Sezione di Ferrara, I-44122, Ferrara, Italy; (B)University of Ferrara, I-44122, Ferrara, Italy*

²⁵ *Institute of Modern Physics, Lanzhou 730000, People's Republic of China*

²⁶ *Institute of Physics and Technology, Peace Ave. 54B, Ulaanbaatar 13330, Mongolia*

²⁷ *Jilin University, Changchun 130012, People's Republic of China*

²⁸ *Johannes Gutenberg University of Mainz, Johann-Joachim-Becher-Weg 45, D-55099 Mainz, Germany*

²⁹ *Joint Institute for Nuclear Research, 141980 Dubna, Moscow region, Russia*

³⁰ *Justus-Liebig-Universitaet Giessen, II. Physikalisches Institut, Heinrich-Buff-Ring 16, D-35392 Giessen, Germany*

³¹ *Lanzhou University, Lanzhou 730000, People's Republic of China*

³² *Liaoning Normal University, Dalian 116029, People's Republic of China*

³³ *Liaoning University, Shenyang 110036, People's Republic of China*

³⁴ *Nanjing Normal University, Nanjing 210023, People's Republic of China*

³⁵ *Nanjing University, Nanjing 210093, People's Republic of China*

³⁶ *Nankai University, Tianjin 300071, People's Republic of China*

³⁷ *National Centre for Nuclear Research, Warsaw 02-093, Poland*

³⁸ *North China Electric Power University, Beijing 102206, People's Republic of China*

³⁹ *Peking University, Beijing 100871, People's Republic of China*

⁴⁰ *Qufu Normal University, Qufu 273165, People's Republic of China*

⁴¹ *Shandong Normal University, Jinan 250014, People's Republic of China*

⁴² *Shandong University, Jinan 250100, People's Republic of China*

⁴³ *Shanghai Jiao Tong University, Shanghai 200240, People's Republic of China*

⁴⁴ *Shanxi Normal University, Linfen 041004, People's Republic of China*

- ⁴⁵ Shanxi University, Taiyuan 030006, People's Republic of China
- ⁴⁶ Sichuan University, Chengdu 610064, People's Republic of China
- ⁴⁷ Soochow University, Suzhou 215006, People's Republic of China
- ⁴⁸ South China Normal University, Guangzhou 510006, People's Republic of China
- ⁴⁹ Southeast University, Nanjing 211100, People's Republic of China
- ⁵⁰ State Key Laboratory of Particle Detection and Electronics, Beijing 100049, Hefei 230026, People's Republic of China
- ⁵¹ Sun Yat-Sen University, Guangzhou 510275, People's Republic of China
- ⁵² Suranaree University of Technology, University Avenue 111, Nakhon Ratchasima 30000, Thailand
- ⁵³ Tsinghua University, Beijing 100084, People's Republic of China
- ⁵⁴ Turkish Accelerator Center Particle Factory Group, (A)Istinye University, 34010, Istanbul, Turkey; (B)Near East University, Nicosia, North Cyprus, Mersin 10, Turkey
- ⁵⁵ University of Chinese Academy of Sciences, Beijing 100049, People's Republic of China
- ⁵⁶ University of Groningen, NL-9747 AA Groningen, The Netherlands
- ⁵⁷ University of Hawaii, Honolulu, Hawaii 96822, USA
- ⁵⁸ University of Jinan, Jinan 250022, People's Republic of China
- ⁵⁹ University of Manchester, Oxford Road, Manchester, M13 9PL, United Kingdom
- ⁶⁰ University of Minnesota, Minneapolis, Minnesota 55455, USA
- ⁶¹ University of Muenster, Wilhelm-Klemm-Str. 9, 48149 Muenster, Germany
- ⁶² University of Oxford, Keble Rd, Oxford, UK OX13RH
- ⁶³ University of Science and Technology Liaoning, Anshan 114051, People's Republic of China
- ⁶⁴ University of Science and Technology of China, Hefei 230026, People's Republic of China
- ⁶⁵ University of South China, Hengyang 421001, People's Republic of China
- ⁶⁶ University of the Punjab, Lahore-54590, Pakistan
- ⁶⁷ University of Turin and INFN, (A)University of Turin, I-10125, Turin, Italy; (B)University of Eastern Piedmont, I-15121, Alessandria, Italy; (C)INFN, I-10125, Turin, Italy
- ⁶⁸ Uppsala University, Box 516, SE-75120 Uppsala, Sweden
- ⁶⁹ Wuhan University, Wuhan 430072, People's Republic of China
- ⁷⁰ Xinyang Normal University, Xinyang 464000, People's Republic of China
- ⁷¹ Yunnan University, Kunming 650500, People's Republic of China
- ⁷² Zhejiang University, Hangzhou 310027, People's Republic of China
- ⁷³ Zhengzhou University, Zhengzhou 450001, People's Republic of China
- ^a Also at the Moscow Institute of Physics and Technology, Moscow 141700, Russia
- ^b Also at the Novosibirsk State University, Novosibirsk, 630090, Russia
- ^c Also at the NRC "Kurchatov Institute", PNPI, 188300, Gatchina, Russia
- ^d Currently at Istanbul Arel University, 34295 Istanbul, Turkey
- ^e Also at Goethe University Frankfurt, 60323 Frankfurt am Main, Germany
- ^f Also at Key Laboratory for Particle Physics, Astrophysics and Cosmology, Ministry of Education; Shanghai Key Laboratory for Particle Physics and Cosmology; Institute of Nuclear and Particle Physics, Shanghai 200240, People's Republic of China
- ^g Also at Key Laboratory of Nuclear Physics and Ion-beam Application (MOE) and Institute of Modern Physics, Fudan University, Shanghai 200443, People's Republic of China
- ^h Also at State Key Laboratory of Nuclear Physics and Technology, Peking University, Beijing 100871, People's Republic of China
- ⁱ Also at School of Physics and Electronics, Hunan University, Changsha 410082, China
- ^j Also at Guangdong Provincial Key Laboratory of Nuclear Science, Institute of Quantum Matter, South China Normal University, Guangzhou 510006, China
- ^k Also at Frontiers Science Center for Rare Isotopes, Lanzhou University, Lanzhou 730000, People's Republic of China
- ^l Also at Lanzhou Center for Theoretical Physics, Lanzhou University, Lanzhou 730000, People's Republic of China
- ^m Also at the Department of Mathematical Sciences, IBA, Karachi, Pakistan

(Dated: April 19, 2022)

Using 448 million $\psi(2S)$ events, the spin-singlet P -wave charmonium state $h_c(1^1P_1)$ is studied via the $\psi(2S) \rightarrow \pi^0 h_c$ decay followed by the $h_c \rightarrow \gamma \eta_c$ transition. The branching fractions are measured to be $\mathcal{B}_{\text{Inc}}(\psi(2S) \rightarrow \pi^0 h_c) \times \mathcal{B}_{\text{Tag}}(h_c \rightarrow \gamma \eta_c) = (4.17_{-0.25}^{+0.27} \pm 0.19) \times 10^{-4}$, $\mathcal{B}_{\text{Inc}}(\psi(2S) \rightarrow \pi^0 h_c) = (7.23 \pm 0.33 \pm 0.38) \times 10^{-4}$, and $\mathcal{B}_{\text{Tag}}(h_c \rightarrow \gamma \eta_c) = (57.66_{-3.50}^{+3.62} \pm 0.58)\%$, where the uncertainties are statistical and systematic, respectively. The $h_c(1^1P_1)$ mass and width are determined to be $M = (3525.32 \pm 0.06 \pm 0.15) \text{ MeV}/c^2$ and $\Gamma = (0.78_{-0.24}^{+0.27} \pm 0.12) \text{ MeV}$.

Using the center of gravity mass of the three $\chi_{cJ}(1^3P_J)$ mesons ($M(\text{c.o.g.})$), the $1P$ hyperfine mass splitting is estimated to be $\Delta_{\text{hyp}} = M(h_c) - M(\text{c.o.g.}) = (0.03 \pm 0.06 \pm 0.15) \text{ MeV}/c^2$, which is consistent with the expectation that the $1P$ hyperfine splitting is zero at the lowest-order.

I. INTRODUCTION

Despite extensive studies of the charmonium system since its discovery in 1974 [1–4], knowledge of the singlet state $h_c(1^1P_1)$ is sparse. Only nine decay modes have been observed, with the $h_c \rightarrow \gamma\eta_c$ predominant, with a branching fraction of $(50 \pm 9)\%$ [5]. And although several measurements of its mass have been performed, more precision is desirable. This would allow better tests of the hypothesis of zero spin-spin hyperfine mass splitting relative to the center-of-gravity mass of the three $\chi_{cJ}(1^3P_J)$ states, defined as [6]

$$M(\text{c.o.g.}) = \frac{M(\chi_{c0}) + 3M(\chi_{c1}) + 5M(\chi_{c2})}{9},$$

where the $M(\chi_{cJ})$ are the masses of the $\chi_{cJ}(1^3P_J)$ states. Only one measurement of the $h_c(1^1P_1)$ width exists, provided by the BESIII experiment based on 106 million $\psi(2S)$ events [7]. The dataset used in the current analysis includes that sample.

A more precise knowledge of the $h_c(1^1P_1)$ resonance parameters is also important given the recent discoveries in the XYZ (charmonium-like) sector with the h_c resonance as an intermediate state. Indeed, BESIII observed the $Z_c^\pm(4020)$ decaying to $\pi^\pm h_c$ [8] as well as two resonant structures in the cross section for $e^+e^- \rightarrow \pi^+\pi^-h_c$ [9]. The signal decays of these exotic states all employ the tagged channel $h_c \rightarrow \gamma\eta_c, \eta_c \rightarrow \text{hadrons}$. Thus, decreasing the uncertainty on the h_c branching fractions and resonance parameters is of the utmost importance.

This article reports an improved determination of the $h_c(1^1P_1)$ resonance parameters taking advantage of $(448.1 \pm 2.9) \times 10^6$ $\psi(2S)$ collected by the BESIII detector in 2009 and 2012 [10]. The mass and width are extracted by studying the $\psi(2S) \rightarrow \pi^0 h_c \rightarrow (\gamma\gamma)(\gamma\eta_c)$ process following the same approach as Ref. [11]. In particular, this study uses the π_0 recoil mass distribution to reconstruct the $h_c(1^1P_1)$ mass, both inclusively ($\psi(2S) \rightarrow \pi^0 h_c$) and by tagging the decay via the electric dipole (E1) transition photon from $h_c \rightarrow \gamma\eta_c$. For the rest of this article, the two data samples will be referred as inclusive and tagged (Inc or Tag as a subscript), respectively. The choice of using two channels is motivated by the necessity of measuring the branching

fractions $\mathcal{B}_{\text{Inc}}(\psi(2S) \rightarrow \pi^0 h_c)$ and $\mathcal{B}_{\text{Tag}}(h_c \rightarrow \gamma\eta_c)$, the uncertainties of which are still large [5].

II. BESIII DETECTOR AND DATASETS

The BESIII detector [12] records symmetric e^+e^- collisions provided by the BEPCII storage ring [13], which operates in the center-of-mass energy range from 2.0 to 4.9 GeV. BESIII has collected large data samples in this energy region [14]. The cylindrical core of the BESIII detector covers 93% of the full solid angle and consists of a helium-based multilayer drift chamber (MDC), a plastic scintillator time-of-flight system (TOF), and a CsI(Tl) electromagnetic calorimeter (EMC), which are all enclosed in a superconducting solenoidal magnet providing a 1.0 T magnetic field. The solenoid is supported by an octagonal flux-return yoke with resistive plate counter muon identification modules interleaved with steel. The charged-particle momentum resolution at 1 GeV/c is 0.5%, and the dE/dx resolution is 6% for electrons from Bhabha scattering. The EMC measures photon energies with a resolution of 2.5% (5%) at 1 GeV in the barrel (end cap) region. The time resolution in the TOF barrel region is 68 ps, while in the end cap is 110 ps.

Simulated data samples produced with a GEANT4-based [15] Monte Carlo (MC) package, which includes the geometric description of the BESIII detector and the detector response, are used to determine detection efficiencies and to estimate backgrounds. The simulation models the beam energy spread and initial state radiation (ISR) in the e^+e^- annihilations with the generator KKMC [16, 17]. The inclusive MC sample consists of the production of the $\psi(2S)$ resonance, the ISR production of the J/ψ , and the continuum processes ($e^+e^- \rightarrow e^+e^-$, $e^+e^- \rightarrow \text{hadrons}$, and $e^+e^- \rightarrow \gamma\gamma$) incorporated in KKMC. The known decay modes are modelled with EVTGEN [18, 19] using branching fractions taken from the Particle Data Group (PDG) [5], and the remaining unknown charmonium decays are modelled with LUNDCHARM [20, 21]. Final state radiation (FSR) from charged final state particles is incorporated using the PHOTOS [22] package. In the signal MC samples, the $\psi(2S) \rightarrow \pi^0 h_c$ decay and the E1 transition $h_c \rightarrow \gamma\eta_c$ are both generated by EVTGEN.

III. EVENT SELECTION AND ANALYSIS PROCEDURE

Although charged tracks are not directly used in the reconstruction, candidate events must have at least two good tracks to suppress background. Good tracks reconstructed in the MDC must pass the following fiducial and production vertex cuts. Only tracks with momenta less than 2.0 GeV/c are considered and they are required to satisfy $|\cos\theta| < 0.93$, where θ is the angle between the momentum and beam axis. The distance of closest approach to the interaction point must be less than 10 cm along the beam axis, and less than 1 cm in the transverse plane. Photon candidates are identified using showers in the EMC. The deposited energy of each shower must be more than 25 MeV in the barrel region ($|\cos\theta| < 0.80$) and more than 50 MeV in the end cap region ($0.86 < |\cos\theta| < 0.92$). To suppress electronic noise and showers unrelated to the event, the difference between the EMC time and the event start time is required to be within (0, 700) ns. To exclude showers that originate from charged tracks, the angle between the position of each shower in the EMC and the closest extrapolated charged track must be greater than 10° . Finally, to suppress the background contribution from the continuum processes, such as Bhabha scattering, the total energy deposit in the EMC ($E_{\text{EMC}}^{\text{Tot}}$) is required to satisfy $0.6 < E_{\text{EMC}}^{\text{Tot}} < 3.2$ GeV. Candidate events are required to have at least two (three) photon candidates passing the fiducial and energy cuts for the inclusive (tagged) channel. The π^0 candidate is reconstructed via its decay to $\gamma\gamma$, with both photon candidates laying in the barrel ($|\cos\theta| < 0.80$) and having an energy ≥ 40 MeV. The di-photon pair is accepted as a π^0 candidate if its invariant mass satisfies $120 < M_{\gamma\gamma} < 145$ MeV/c². Multiple π^0 candidates are allowed in one event. A one-constraint (1C) kinematic fit fixing the π^0 mass to its known value [5] is used to improve the energy resolution. Candidates with a fit $\chi^2 > 200$ are rejected. The dominant background for the inclusive sample comes from combining photons from two different π^0 s; the shape of this background is discussed below. The photon coming from the E1 decay (γ_{Tag}) is expected to peak around 500 MeV. Taking into consideration that $\Gamma_{\eta_c} \approx 30$ MeV [5], the E1 photon is required to satisfy $465 < E_{\gamma_{\text{Tag}}} < 535$ MeV and must not form a π^0 with any other photons in the event. In the tagged channel, if more than one π^0 is found in the π^0 recoil mass signal region (3.500–3.550 GeV/c²) the π^0 with the minimum 1C fit χ^2 is kept.

The three main background sources are $\psi(2S) \rightarrow J/\psi \pi^+ \pi^-$, $\psi(2S) \rightarrow J/\psi \pi^0 \pi^0$, and $\psi(2S) \rightarrow \gamma \chi_{c0}$. The

first two are suppressed by requiring all combinations of the $\pi^+ \pi^-$ ($\pi^0 \pi^0$) recoil mass to be outside the range $M_{J/\psi} \pm 4$ MeV/c² ($M_{J/\psi} \pm_{-8}^{+38}$ MeV/c²), where $M_{J/\psi}$ is the nominal J/ψ mass [5]. This veto window is optimized based on the figure of merit $\frac{S}{\sqrt{S+B}}$, where S and B are the numbers of signal and background events estimated from the MC. No suppression of the $\gamma \chi_{c0}$ decay is needed since the photon energy is not in the tagged photon energy range, and thus this decay contributes to the background with a typical combinatorial shape.

The signal efficiencies, $\epsilon_{\text{Tag}} = 12.37\%$ and $\epsilon_{\text{Inc}} = 14.25\%$, are estimated for the tagged and inclusive channels, respectively, based on two signal MC samples of 300000 events each. The signal shape is modeled with a resolution function (shown in Fig. 1) based on MC. It is a sum of a Gaussian function and a Crystal Ball function; both contribute to symmetric smearing while the latter also includes the low-energy tail due to π^0 reconstruction. The parameters of this resolution function are obtained from a signal MC dataset where the $h_c(1^1P_1)$ width is set to 0. The convolution of the resolution function and a Breit-Wigner distribution is used to describe the signal in the final dataset to extract N_{Inc} and N_{Tag} (i.e., the number of the inclusive and tagged events, respectively). Defining $N(\psi(2S))$ as the total number of $\psi(2S)$ events, the various branching fractions, \mathcal{B} , are obtained as

$$\begin{aligned} \bullet \mathcal{B}_{\text{Inc}}(\psi(2S) \rightarrow \pi^0 h_c) &= \frac{N_{\text{Tag}}}{\epsilon_{\text{Tag}} \times N(\psi(2S))}; \\ \bullet \mathcal{B}_{\text{Inc}}(\psi(2S) \rightarrow \pi^0 h_c) &= \frac{N_{\text{Inc}}}{\epsilon_{\text{Inc}} \times N(\psi(2S))}; \\ \bullet \mathcal{B}_{\text{Tag}}(h_c \rightarrow \gamma \eta_c) &= \frac{\mathcal{B}_{\text{Inc}}(\psi(2S) \rightarrow \pi^0 h_c) \times \mathcal{B}_{\text{Tag}}(h_c \rightarrow \gamma \eta_c)}{\mathcal{B}_{\text{Inc}}(\psi(2S) \rightarrow \pi^0 h_c)} = \\ &= \frac{N_{\text{Tag}} \times \epsilon_{\text{Inc}}}{N_{\text{Inc}} \times \epsilon_{\text{Tag}}}. \end{aligned}$$

To assess the shape of the irreducible background, a MC dataset (described in Sec. II) of 400 million inclusive $\psi(2S)$ decays with the signal contributions are removed is studied. This shows that a 5th-order Chebychev polynomial satisfactorily describes the irreducible background in both the channels.

Fits to the distributions of the π^0 recoil mass are performed minimizing the negative log-likelihood on the inclusive and tagged channels separately. The total probability function is constructed from a 5th-order Chebychev polynomial, to describe the background, added to a convolution of the resolution function and a Breit-Wigner distribution for the signal. In the tagged channel, the parameters of the Chebychev polynomial are allowed to

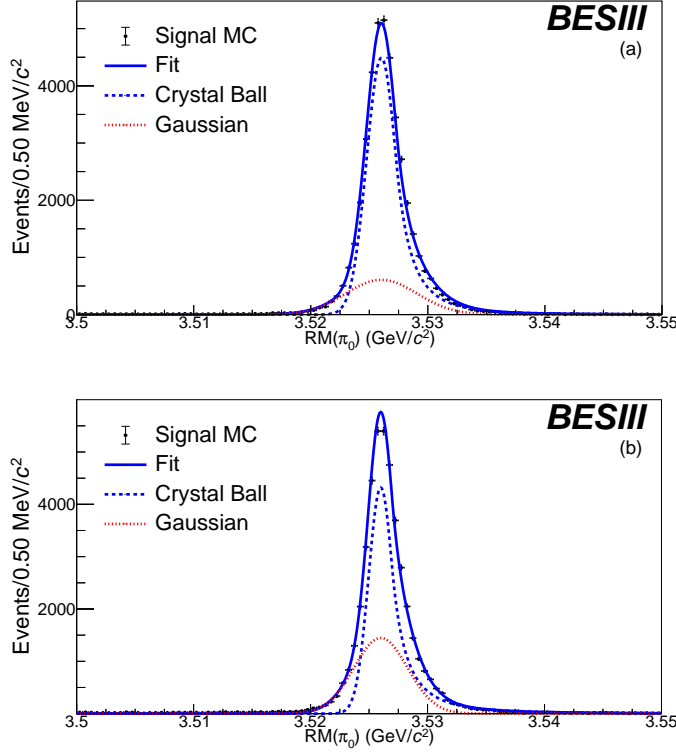


FIG. 1. Signal MC π_0 recoil mass (referred as $RM(\pi_0)$) distributions for the $h_c(1^1P_1)$ with its width set to 0. The solid blue line refers to the global fit result, while the black dots with error bars are the MC simulation. The blue dashed line represents the Crystal Ball component, while the red dotted one is the Gaussian component. Fig. (a) shows the resolution function for the inclusive channel, while the one for the tagged chain is presented in Fig. (b).

float, as well as the mass and the width of the $h_c(1^1P_1)$ resonance. But for the inclusive channel, the signal shape parameters are fixed to the values found in the tagged channel, while the parameters of the Chebychev polynomial are left floating. Tests on MC samples are used to validate both the model and the fitting procedure; no bias is found.

The fit results are summarized in Table I. A comparison between this analysis and the PDG[5] shows compatibility between the central values with improved precision. Fig. 2 presents the fits for the π^0 recoil mass spectra, $RM(\pi_0)$, for both the inclusive and tagged channels. Separate fits to the 2009 and 2012 datasets yield parameters compatible with each other within 1.5σ . The systematic uncertainties reported in Table I are described in detail in the next section.

TABLE I. Results of the fits to the π^0 recoiling mass spectra with statistical (first) and systematic (second) uncertainties. The last column provides current PDG values.

Variable	Value	PDG Value [5]
$M(h_c)$ (MeV/ c^2)	$3525.32 \pm 0.06 \pm 0.15$	3525.38 ± 0.11
$\Gamma(h_c)$ (MeV)	$0.78^{+0.27}_{-0.24} \pm 0.12$	0.7 ± 0.4
$N_{\text{Tag}}(h_c)$	23118^{+1500}_{-1398}	—
$\mathcal{B}_{\text{Inc}} \times \mathcal{B}_{\text{Tag}} (10^{-4})$	$4.17^{+0.27}_{-0.25} \pm 0.19$	4.58 ± 0.64 (BESIII [11]) 4.16 ± 0.48 (CLEO [23])
$N_{\text{Inc}}(h_c)$	46187 ± 2123	—
$\mathcal{B}_{\text{Inc}} (10^{-4})$	$7.23 \pm 0.33 \pm 0.38$	8.60 ± 1.30
$\mathcal{B}_{\text{Tag}} (\%)$	$57.66^{+3.62}_{-3.50} \pm 0.58$	50 ± 9

IV. SYSTEMATIC UNCERTAINTIES

Sources of systematic uncertainties on the measurement of the $h_c(1^1P_1)$ resonance parameters and branching fractions include the background line-shape, the mass ranges for the veto of J/ψ from $\psi(2S)$, the photon energy calibration and reconstruction efficiency, the π^0 reconstruction efficiency, and the luminosity. The contributions from each source are shown in Table II. For each measurement, the total systematic uncertainty corresponds to a quadrature sum of all individual sources, which are discussed in detail next.

Background line-shape. To determine the systematic uncertainties associated to the fit function, a 4th-order Chebychev polynomial to describe the background behaviour in both the inclusive and tagged channels is tested. The discrepancy with respect to the nominal fit result is taken as a systematic uncertainty. Assuming that part of the background events might be miscounted as signal, a first-order polynomial is added to the resolution function, maintaining a 4th order Chebychev polynomial to describe the main background contribution. The discrepancy between this method and the nominal one is taken as a systematic uncertainty and summed in quadrature with the result from the first variation.

Mass ranges for the veto of J/ψ from $\psi(2S)$. Mass veto ranges for the $\pi^0\pi^0$ and $\pi^+\pi^-$ recoiling masses are changed according to the observed variations of the figure of merit. Two different scenarios are tested,

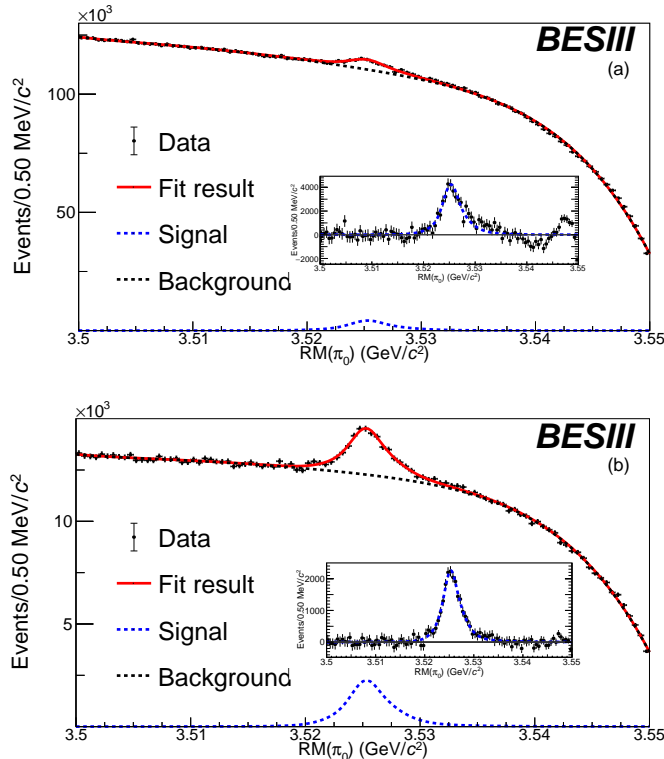


FIG. 2. Fits to the π^0 recoil mass spectra for the (a) inclusive and (b) tagged samples. Red solid lines denote the fit results, while the black dots with error bars are the data. The blue dashed lines represent the signal component and the black dashed lines are the background. Insets show the background-subtracted data with the signal shape overlaid.

- for the $\pi^+ \pi^- J/\psi$ background, $M_{J/\psi} \pm 3 \text{ MeV}/c^2$ and $M_{J/\psi} \pm 5 \text{ MeV}/c^2$;
- for the $\pi^0 \pi^0 J/\psi$ background, $M_{J/\psi}^{+37}_{-7} \text{ MeV}/c^2$ and $M_{J/\psi}^{+39}_{-9} \text{ MeV}/c^2$.

In both cases, smaller veto ranges give the largest changes with respect to the nominal vetoes; these changes are taken as systematic uncertainties.

Photon reconstruction efficiency. The systematic uncertainties arising from potential inconsistencies of the photon-energy measurements between data and MC simulation are obtained from Ref. [7].

Photon energy calibration. The uncertainty due to the photon energy distribution is obtained from Ref. [7].

TABLE II. Summary of the systematic uncertainties on the $h_c(1^1P_1)$ resonance parameters and branching fractions, in percent. The — symbol is used when the systematic sources are found to be negligible or not applicable. For each measurement, the total systematic uncertainty corresponds to a quadrature sum of all individual contributions.

Source	$M(h_c)$	$\Gamma(h_c)$	$\mathcal{B}_{\text{Inc}} \times \mathcal{B}_{\text{Tag}}$	\mathcal{B}_{Inc}	\mathcal{B}_{Tag}
Background shape	0.002	—	0.34	2.27	—
J/ψ veto	0.001	9.33	3.12	4.21	—
γ reconstruction efficiency	—	—	3.00	2.00	1.00
γ energy calibration	0.004	8.97	—	—	—
Signal shape	—	7.69	—	—	—
π^0 reconstruction efficiency	—	—	1.00	1.00	—
Number of $\psi(2S)$ events	—	—	0.65	0.65	—
Total systematic uncertainty	0.004	15.06	4.50	5.32	1.00

Signal shape. This uncertainty includes contributions from the signal line-shape and the 1-C kinematic fit, and is estimated in Ref. [7].

π^0 reconstruction efficiency. The uncertainty on the branching fractions due to the π^0 reconstruction efficiency is estimated in Ref. [24].

Number of $\psi(2S)$ events. This uncertainty is estimated in Ref. [10], and included in the branching fraction uncertainties.

Other sources of the possible systematic uncertainties are studied, but found to be negligible. These include the bin size, the signal region, the trigger efficiency, the numbers of π^0 and charged tracks, the masses and widths of the $\psi(2S)$ and η_c , and the sample sizes of the MC simulations.

V. RESULTS AND SUMMARY

In this article, two decay chains involving the $h_c(1^1P_1)$ charmonium state are studied,

- inclusive: $\psi(2S) \rightarrow \pi^0 h_c$ with $h_c \rightarrow$ anything,
- tagged: $\psi(2S) \rightarrow \pi^0 h_c$ with $h_c \rightarrow \gamma \eta_c$.

The measurements of the $h_c(1^1P_1)$ resonance parameters and branching fractions are performed with the world's largest $\psi(2S)$ data sample, collected by the BESIII experiment [10]. Table I shows the improved precision of this measurement with respect to the PDG values [5], and compatibility within one standard deviation.

Furthermore, using current PDG [5] values for the center-of-gravity mass of the three $\chi_{cJ}(1^3P_J)$ states, $M(\text{c.o.g.})$, an updated value for the $1P$ hyperfine mass splitting ($\Delta_{\text{hyp}} = M(\text{c.o.g.}) - M(h_c)$) may be obtained. This value is predicted by QCD to be identical to 0 at leading-order [6]. No mass splitting is observed with this measurement,

$$\Delta_{\text{hyp}} = 0.03 \pm 0.06 \text{ (stat.)} \pm 0.15 \text{ (syst.) MeV}/c^2.$$

These results on Δ_{hyp} show that, with the foreseen increase in $\psi(2S)$ statistics by the BESIII experiment [14], significant efforts to reduce systematic uncertainties will be necessary.

Acknowledgements

The BESIII collaboration thanks the staff of BEPCII and the IHEP computing center for their strong sup-

port. This work is supported in part by National Key R&D Program of China under Contracts Nos. 2020YFA0406300, 2020YFA0406400; National Natural Science Foundation of China (NSFC) under Contracts Nos. 11625523, 11635010, 11735014, 11822506, 11835012, 11935015, 11935016, 11935018, 11961141012, 12022510, 12025502, 12035009, 12035013, 12061131003; the Chinese Academy of Sciences (CAS) Large-Scale Scientific Facility Program; Joint Large-Scale Scientific Facility Funds of the NSFC and CAS under Contracts Nos. U1732263, U1832207; CAS Key Research Program of Frontier Sciences under Contract No. QYZDJ-SSW-SLH040; 100 Talents Program of CAS; INPAC and Shanghai Key Laboratory for Particle Physics and Cosmology; ERC under Contract No. 758462; European Union Horizon 2020 research and innovation programme under Contract No. Marie Skłodowska-Curie grant agreement No 894790; German Research Foundation DFG under Contracts Nos. 443159800, Collaborative Research Center CRC 1044, FOR 2359, FOR 2359, GRK 214; Istituto Nazionale di Fisica Nucleare, Italy; Ministry of Development of Turkey under Contract No. DPT2006K-120470; National Science and Technology fund; Olle Engkvist Foundation under Contract No. 200-0605; STFC (United Kingdom); The Knut and Alice Wallenberg Foundation (Sweden) under Contract No. 2016.0157; The Royal Society, UK under Contracts Nos. DH140054, DH160214; The Swedish Research Council; U. S. Department of Energy under Contracts Nos. DE-FG02-05ER41374, DE-SC-0012069.

-
- [1] J. J. Aubert *et al.* (E598 Collaboration), Phys. Rev. Lett. **33**, 1404 (1974).
 [2] J. E. Augustin *et al.* (SLAC-SP-017), Phys. Rev. Lett. **33**, 1406 (1974).
 [3] C. Bacci *et al.*, Phys. Rev. Lett. **33**, 1408 (1974), [Erratum: Phys.Rev.Lett. 33, 1649 (1974)].
 [4] G. S. Abrams *et al.*, Phys. Rev. Lett. **33**, 1453 (1974).
 [5] P. Zyla *et al.* (Particle Data Group), PTEP **2020**, 083C01 (2020).
 [6] W. Kwong, J. L. Rosner, and C. Quigg, Ann. Rev. Nucl. Part. Sci. **37**, 325 (1987).
 [7] M. Ablikim *et al.* (BESIII Collaboration), Phys. Rev. D **86**, 092009 (2012).
 [8] M. Ablikim *et al.* (BESIII Collaboration), Phys. Rev. Lett. **111**, 242001 (2013).
 [9] M. Ablikim *et al.* (BESIII Collaboration), Phys. Rev. Lett. **118**, 092002 (2017).
 [10] M. Ablikim *et al.* (BESIII Collaboration), Chin. Phys. C **42**, 023001 (2018).
 [11] M. Ablikim *et al.* (BESIII Collaboration), Phys. Rev. Lett. **104**, 132002 (2010).
 [12] M. Ablikim *et al.* (BESIII Collaboration), Nucl. Instrum. Methods Phys. Res., Sect. A **614**, 345 (2010).
 [13] C. H. Yu *et al.*, Proceedings of IPAC2016, Busan, Korea (2016), 10.18429/JACoW-IPAC2016-TUYA01.
 [14] M. Ablikim *et al.* (BESIII Collaboration), Chin. Phys. C **44**, 040001 (2020).
 [15] S. Agostinelli *et al.* (GEANT4), Nucl. Instrum. Methods Phys. Res., Sect. A **506**, 250 (2003).
 [16] S. Jadach, B. F. L. Ward, and Z. Was, Phys. Rev. D **63**, 113009 (2001).
 [17] S. Jadach, B. F. L. Ward, and Z. Was, Comput. Phys. Commun. **130**, 260 (2000).
 [18] D. J. Lange, Nucl. Instrum. Methods Phys. Res., Sect. A **462**, 152 (2001).

- [19] R.-G. Ping, Chin. Phys. C **32**, 599 (2008).
- [20] J. C. Chen, G. S. Huang, X. R. Qi, D. H. Zhang, and Y. S. Zhu, Phys. Rev. D **62**, 034003 (2000).
- [21] R.-L. Yang, R.-G. Ping, and H. Chen, Chin. Phys. Lett. **31**, 061301 (2014).
- [22] E. Richter-Was, Phys. Lett. B **303**, 163 (1993).
- [23] S. Dobbs *et al.* (CLEO Collaboration), Phys. Rev. Lett. **101**, 182003 (2008).
- [24] M. Ablikim *et al.* (BESIII Collaboration), Phys. Rev. D **81**, 052005 (2010).